Catena 120 (2014) 111–121

Contents lists available at ScienceDirect

Catena

journal homepage: www.elsevier.com/locate/catena

# Investigation of rainfall–runoff modeling for Egypt by using remote sensing and GIS integration

Shereif H. Mahmoud *

*Alamoudi Water Research Chair, King Saud University, Saudi Arabia*

ARTICLE INFO

*Article history:*
Received 18 December 2013
Received in revised form 9 April 2014
Accepted 14 April 2014
Available online 8 May 2014

*Keywords:*
Potential runoff coefficient (PRC)
Geographical information system (GIS)
Hydrological soil group (HSG)
Digital elevation model (DEM)
Land cover/land use (LCLU)

ABSTRACT

Egypt is characterized as a "water scarce" country, with limited fresh water supplies, and is expected to be under water stress by the year 2030. Therefore, it is important to develop any available means to supply water to maintain human life, such as runoff harvesting approach. The curve number (CN) is a hydrologic parameter used to describe the stormwater runoff potential for drainage areas, and it is a function of land use, soil type, and soil moisture. This study was conducted to estimate the potential runoff coefficient (PRC) using geographic information system (GIS) based on the area's hydrologic soil group (HSG), land use, slope and determine the runoff volume. The soil map of Egypt was extracted from the soil map of the world and then was used in building a soil hydrological group map. Landsat image 5/7 TM/ETM was incorporated with land cover data to generate land use and land cover (LULC) map. Slope map for Egypt was generated from a 30 m DEM. The GIS technique was used to generate PRC map. Annual runoff depth is derived based on the annual rainfall surplus and runoff coefficient per pixel using raster calculator tool in ArcGIS. A variation from as low as 0 to a maximum of 180 mm was observed due to divergence in topography and climate in Egypt where the largest rainfall was observed in the northern part of the country. Generally, the result of this study indicates that in the absence of reliable ground measurements of rainfall, the product can satisfactorily be applied to estimate the spatial rainfall distribution based on values of R and $R^2$ (0.94) obtained.



## 1. Introduction

Egypt has been suffering from severe water scarcity in recent years. Uneven water distribution, misuse of water resources and inefficient irrigation techniques are some of the major factors playing havoc with water security in the country. Being more or less an arid country, Egypt is heavily dependent on rain to support its rapidly growing population and development. The Nile River is the lifeline of the country, as it serves the country's industrial and agricultural demand and is the primary source of drinking water for the population. Rising populations and rapid economic development in the countries of the Nile Basin, pollution and environmental degradation are decreasing water availability for Egypt. Egypt is facing an annual water deficit around 7 billion cubic meters. In fact, United Nations is already warning that Egypt could run out of water by the year 2025.

Rain harvesting is one solution as it represents one of the indispensable water supplies for the sustainability of water, and development means of using this source efficiently. A classic example of water and nutrient harvesting was the delta of the river Nile before the Aswan dam was constructed. The yearly flooding of agricultural fields made permanent agriculture in this arid region possible. After the construction of the dam, this was no longer possible. Now, farmers have, besides advantages of greater water availability, big problems in keeping the land fertile. Small water harvesting systems with an external catchment area are functioning more or less in the same way.

Runoff coefficient is defined as the portion of rainfall that becomes direct runoff during an event. The concept of event runoff coefficients dates back to the beginning of the 20th century (Sherman, 1932). The runoff coefficient can be defined either as the ratio of the total depth of runoff to a total depth of rainfall, or as the ratio of the peak rate of runoff to rainfall intensity for the time of concentration (Wanielista and Yousef, 1993). Runoff coefficients can be used in event-based derived flood frequency models (Sivapalan et al., 2005) for estimating flood occurrences from rainfall frequencies. These coefficients are useful for understanding the flood frequency controls in a particular hydrologic or climatic regime. At the time rainfall-producing runoff occurs, the coefficient varies with topography, land use, vegetal cover, soil type, and moisture content of the soil (Texas Department of Transportation, TxDOT, 2002). The rational runoff coefficient is strongly dependent on land use and to a lesser extent by watershed slope, as suggested by American Society of Civil Engineers (ASCE) (1992).

The runoff curve number (CN) is an empirical parameter used in hydrology for predicting direct runoff or infiltration from rainfall excess.

* Corresponding author.
*E-mail address:* eng.shereif1@hotmail.com.

http://dx.doi.org/10.1016/j.catena.2014.04.011
0341-8162/

The USDA Natural Resources Conservation Service, which was formerly called the Soil Conservation Service or SCS, developed the curve number method — the number is still popularly known as an "SCS runoff curve number" in the literature. The runoff curve number was developed from an empirical analysis of runoff from small catchments and hill slope plots as monitored by the USDA.

The runoff curve number is based on the area's hydrologic soil group, land use, treatment and hydrologic condition. References, such as from USDA indicate the runoff curve numbers for characteristic land cover descriptions and a hydrologic soil group. The basic assumption of the SCS curve number method is that, for a single storm, the ratio of actual soil retention after runoff begins to potential maximum retention is equal to the ratio of direct runoff to available rainfall.

The GIS has become a critical tool in hydrological modeling because of its capacity to handle large amount of spatial and attribute data. Some of its features, such as map overlay and analysis, help for deriving and aggregating hydrologic parameters from different sources such as soil, land cover, and rainfall data (Cheng et al., 2006; De Winnaar et al., 2007).

In flood prediction and rainfall–runoff computation, physically based distributed hydrological models have become a more feasible approach in recent years (Liu, 2004). The authors stated that in addition to the development of improved computational capabilities, DEMs, digital data of soil type, land use, and the tools of GIS, there are new possibilities for hydrological research in understanding the fundamental physical processes underlying the hydrological cycle, and solution of the mathematical equations representing those processes. Runoff coefficient data for Egypt are not available so far, as well as the experimental data are limited; therefore the assignment of the runoff coefficient (RC) is somewhat subjective.

The main objective of this research work was to:

- Determine the potential runoff coefficient, runoff depth, and runoff modeling for Egypt using GIS, available data and remote sensing.

## 2. Methodology

Implementation of this study required distinctive efforts in different fields or disciplines. In addition to office work, a field survey, an assortment of supporting techniques such as the use of GIS, and satellite images were conducted. These efforts and techniques were utilized for identifying potential runoff coefficient. The following are the materials and software used in the implementation of this study. The materials included were ESRI ArcGIS and Spatial Analyst Extension, ERDAS IMAGINE, and satellite imagery. The following are the main collected data which have been used:

1. Soil texture map
2. Digital elevation model
3. Ground truth point for land cover generation
4. TM and ETM Landsat satellite imagery for Egypt region for 2000
5. GPS ground truth points.
6. Rainfall data.

The methodology followed in determining the potential runoff coefficient for the study area using GIS is shown in Fig. 1.

### 2.1. The study area

This study was to model the runoff due to the rainfall — for Egypt, using the remote sensing and GIS integration. Egypt lies in the northeastern corner of the African continent (Fig. 2) and has a total area of about 1 million square kilometers ($km^2$). The Egyptian terrain consists of a vast desert plateau interrupted by the Nile Valley and Delta, which occupy about 4% of the total country area. The land surface rises on both sides of the valley reaching about 1000 m above sea level in the east and about 800 m above sea level in the west. The highest point of the country, at Mount Catherine in Sinai, is 2629 m above sea level and the lowest point, at the Qattara Depression in the northwest, is 133 m below mean sea level. The majority of the country area is desert land.

Most of the cultivated land is located close to the banks of the Nile River, its main branches and canals, and in the Nile Delta. Rangeland is restricted to a narrow strip, only a few kilometers wide, along the Mediterranean coast and its bearing capacity is quite low. There is no forestland. The total cultivated area (arable land plus permanent crops) is 3.4 million hectares (ha) (2002), or about 3% of the total area of the country. Arable land is about 2.9 million ha, or 85% of the total cultivated area, and permanent crops occupy the remaining 0.5 million ha.

Hot dry summers and mild winters characterize Egypt's climate. Rainfall is very low, irregular and unpredictable. Annual rainfall ranges between a maximum of about 200 mm in the northern coastal region to a minimum of nearly zero in the south, with an annual average of 51 mm. Summer temperatures are extremely high, reaching 38 °C to 43 °C with extremes of 49 °C in the southern and western deserts. The northern areas on the Mediterranean coast are much cooler, with 32 °C as a maximum.

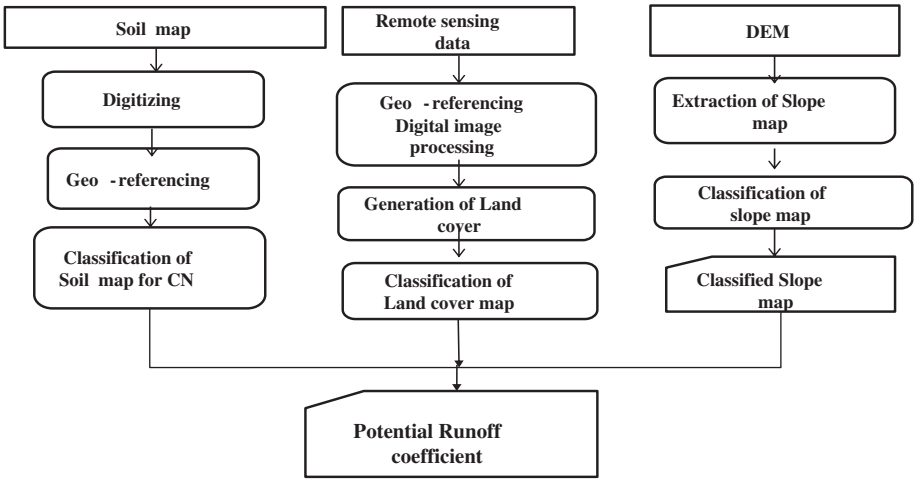


**Fig. 1.** Conceptual framework of runoff coefficient potential mapping (Shereif et al., 2013).

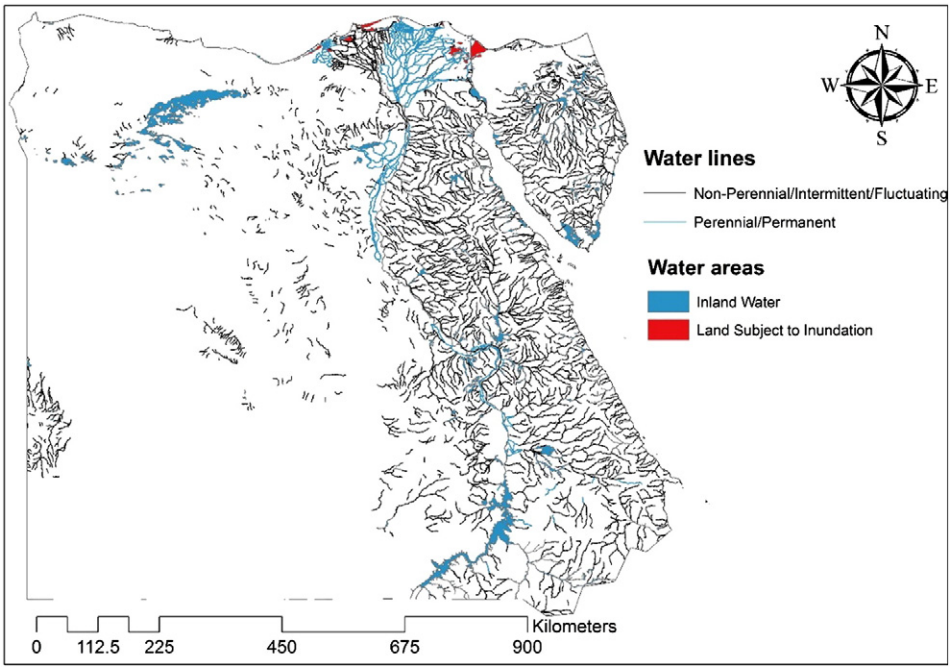


**Fig. 2.** Location map of the studying area.

### 2.2. Soil map

The soil map of Egypt obtained from FAO (1978), which is particularly extracted from the Soil Map of the World. The soil associations are indicated on the original maps by the symbol of the dominant soil unit, followed by a number, which refers to the descriptive legend on the back of the map, where the full composition of the association is given. Associations in which Lithosols are dominant are marked by the Lithosols symbol I combined with one or two associated soil units or inclusions; where there are no associated soils, the symbol I alone is used.

The legend of the original soil map of the World (FAO, 1974) comprises an estimated 4930 different map units, which consist of soil units or associations of soil units. When a map unit is not homogeneous, it is composed of a dominant soil and component soils. The latter are: associated soils, covering at least 20% of the area; and inclusions, important soils which cover less than 20% of the area. The soil map was classified into two classes: loam and sand (Fig. 3). The loamy soil has a moderate infiltration rate when it is thoroughly wetted, and classified as mainly or moderately deep infiltration, moderately to-well drained soils with moderately fine to moderately coarse textures. In addition, sandy soil has the higher infiltration rates.

### 2.3. Land cover and land use

Landsat 5/7 TM/ETM image was incorporated with collected data and ultimately utilized in categorizing land use and land cover (LULC).

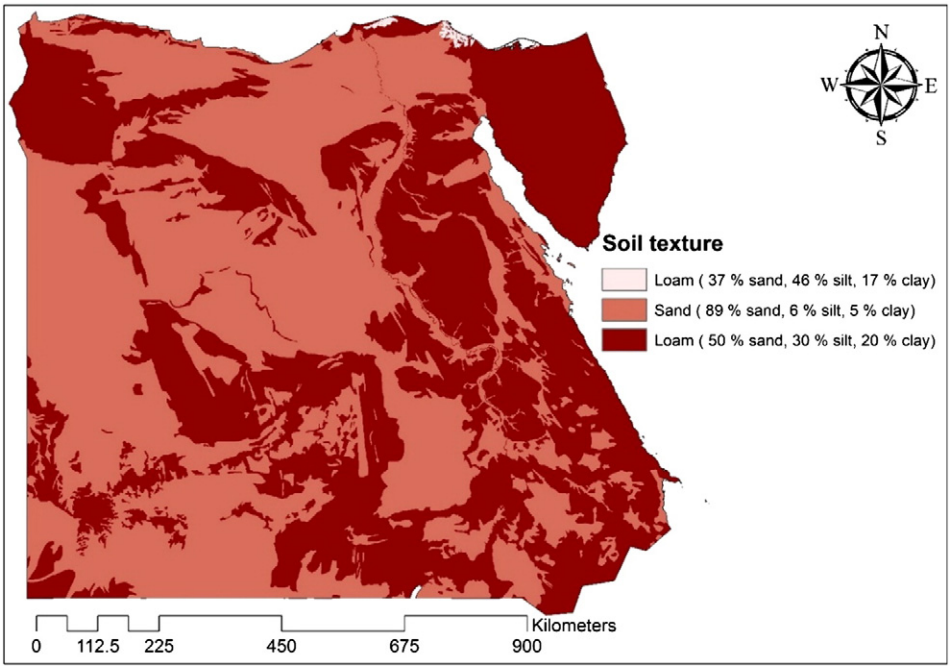


**Fig. 3.** Soil texture map for the study area.

Iso Cluster unsupervised classification and maximum likelihood classification function in the ArcGIS Spatial Analyst was used for the unsupervised classification. Training samples were collected during field survey in addition to collected Landcover data from USGS EROS Data Center to create spectral signatures (i.e., Reflectance values) for the supervised classification to identify what the cluster represents (e.g., Water, bare earth, dry soil, etc.). The LULC map was classified into 15 main classes as shown in Fig. 4. The area covered by each land cover and land use was presented in Table 1.

Table 1 shows the different land cover and land use classes in the study area where barren or sparsely vegetated land represents the largest ratio of the area 95.03%, and 2.08% of the total area are irrigated cropland and pasture. Water bodies as shown in Table 1, represent 0.62% of the total area which are fixed sources.

**Table 1**
Areas covered by the different land cover and land use.

| Class number | Class name | Area ($km^2$) | % of total area |
|---|---|---|---|
| 1 | Barren or sparsely vegetated | 950,288 | 95.03 |
| 2 | Cropland/grassland mosaic | 1864 | 0.19 |
| 3 | Cropland/woodland mosaic | 330 | 0.03 |
| 4 | Deciduous broadleaf forest | 163 | 0.02 |
| 5 | Dryland cropland and pasture | 4386 | 0.44 |
| 6 | Evergreen broadleaf forest | 2133 | 0.21 |
| 7 | Evergreen needle leaf forest | 40 | 0.00 |
| 8 | Grassland | 4286 | 0.43 |
| 9 | Irrigated cropland and pasture | 20,756 | 2.08 |
| 10 | Mixed shrubland/grassland | 2641 | 0.26 |
| 11 | Mixed tundra | 1 | 0.00 |
| 12 | Savanna | 2329 | 0.23 |
| 13 | Shrubland | 4111 | 0.41 |
| 14 | Urban and built-up land | 486 | 0.05 |
| 15 | Water bodies | 6217 | 0.62 |

### 2.4. Slope (topography)

Digital elevation model (DEM) of 30 m was used to generate the slope map for Egypt. The DEM was analyzed to remove sinks and flat areas to maintain continuity of flow to the catchment outlets. GIS was used for DEM preparation by filling the sink areas so the DEM is ready for the next step as presented in Fig. (5). Slope map (Fig. 6) was generated from Egypt filled DEM.

### 2.5. Potential runoff coefficient

The curve number (CN) is a hydrologic parameter used to describe the storm water runoff potential for drainage area, and it is a function of land use, soil type, and soil moisture. Shereif et al. (2013) conducted a study to determine the potential runoff coefficient in Al-Baha region, Saudi Arabia using RS and GIS. The satellite imagery of the Al-Baha region was used in addition to land cover/use map, and soil map.

In this study in order to estimate the potential runoff coefficient (PRC) using GIS based on the area's hydrologic soil group, land use, and slope map were reclassified in groups as follows:

1. Land cover map was reclassified into four main classes (forest, grass and shrub, cropland and bare soil); these groups were given weight values of 100, 200, 300, and 400 respectably (Fig. 7).
2. Soil texture (type) map was used to build a soil hydrological group map and this group given values 1000, 2000, and 3000 for the 3 classes (Fig. 8).
3. Slope map also, was reclassified into four classes and then given values from one to four (Fig. 9).

GIS was used to combine the last three maps into one map then a new field was added to the attribute table of the CN values. These values were inserted into the map from the potential runoff coefficient in Table 3. The potential runoff coefficients for impervious (including open water surface) were set to 1. In addition, surface slope was discretized into four classes as shown in Table 2. Values in the table are taking from the published materials in different references from the literature (Browne, 1990; Chow et al., 1988; Fetter, 1980; Kirkby and Beven, 1979; & Shereif et al., 2013) and adjusted after Mallants and Feyen (1990).

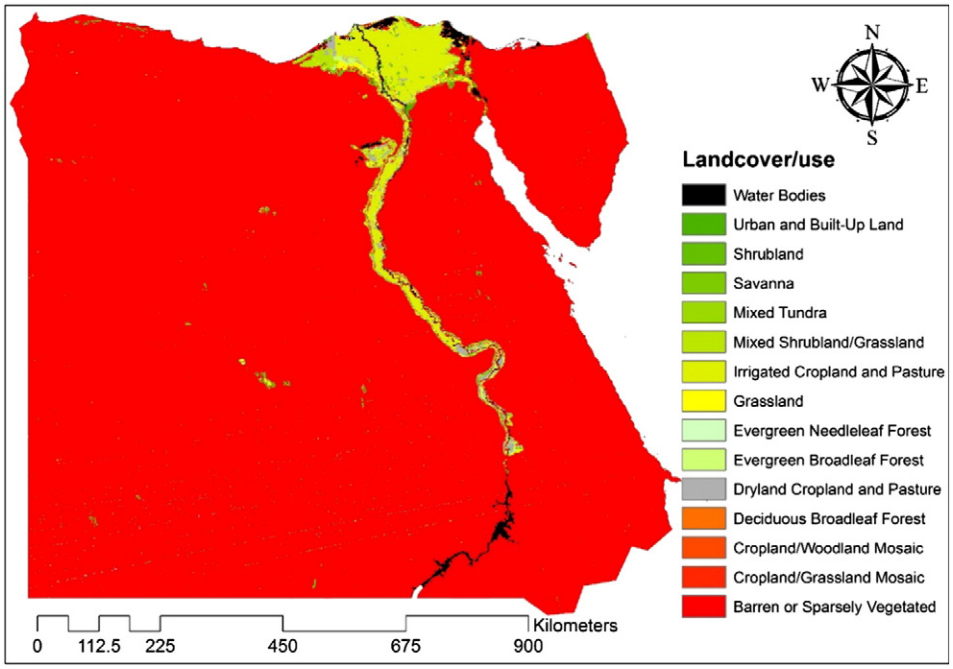


**Fig. 4.** Classified LULC map for Egypt.

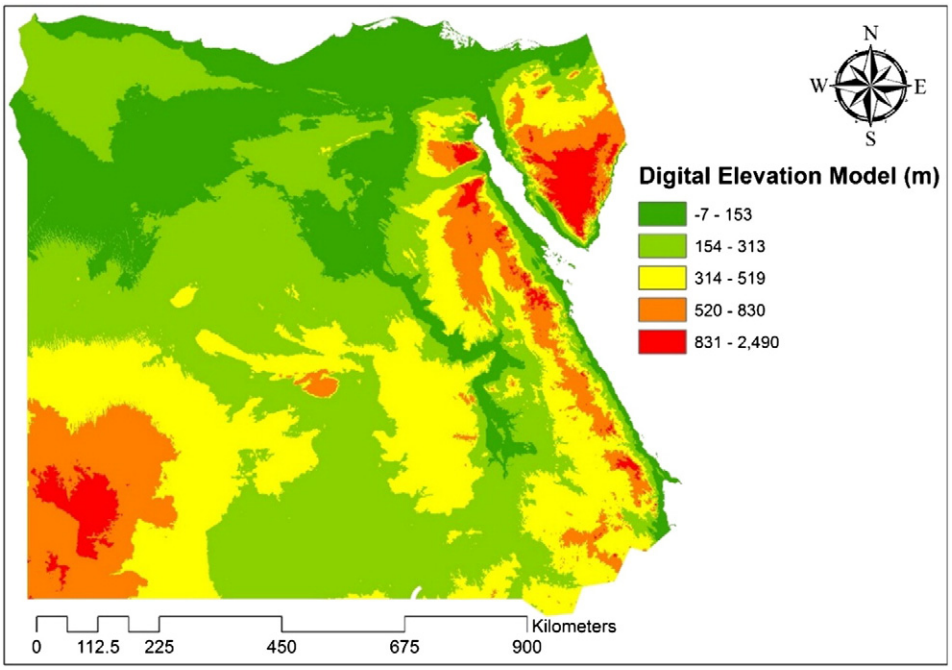


**Fig. 5.** The exploitation of digital elevation model for Egypt.

In order to estimate the potential runoff coefficient based on a continuous slope, a simple linear relationship between potential runoff coefficients and surface slope is used, which can be described by Eq. (1) (Liu and De Smedt, 2004).

$$C = C_0 + (1 - C_0)\frac{S}{S + S_0} \quad (1)$$

where $C$ is the potential runoff coefficient for a surface slope $S$ (%), $C_0$ is the potential runoff coefficient for a near zero slope corresponding to the values listed in the first row of each land use class in Table 2. In addition, $S_0$ (%) is a slope constant for different land use and soil type combinations, which is calibrated using the data in Table 3.

### 2.6. Rainfall surplus

The amount of rainfall at different locations in Egypt was collected for a period of 31 years. The data indicated that rainfall in Egypt is very scarce, with an annual average of 12 mm and ranges from 0 mm/year in the desert to 200 mm/year in the north coastal region. The maximum

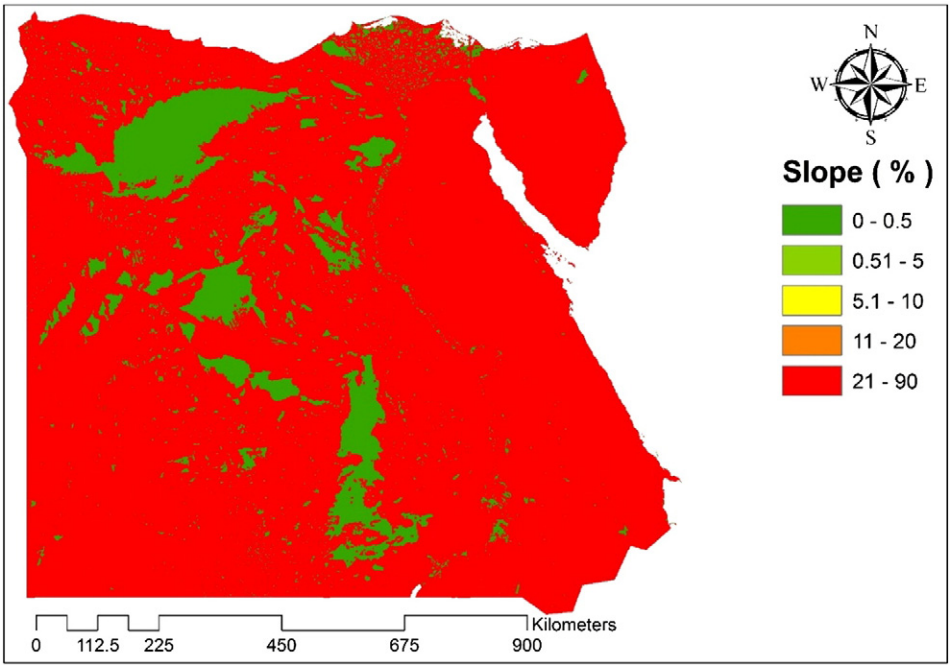


**Fig. 6.** Slope map for determination of PRC.

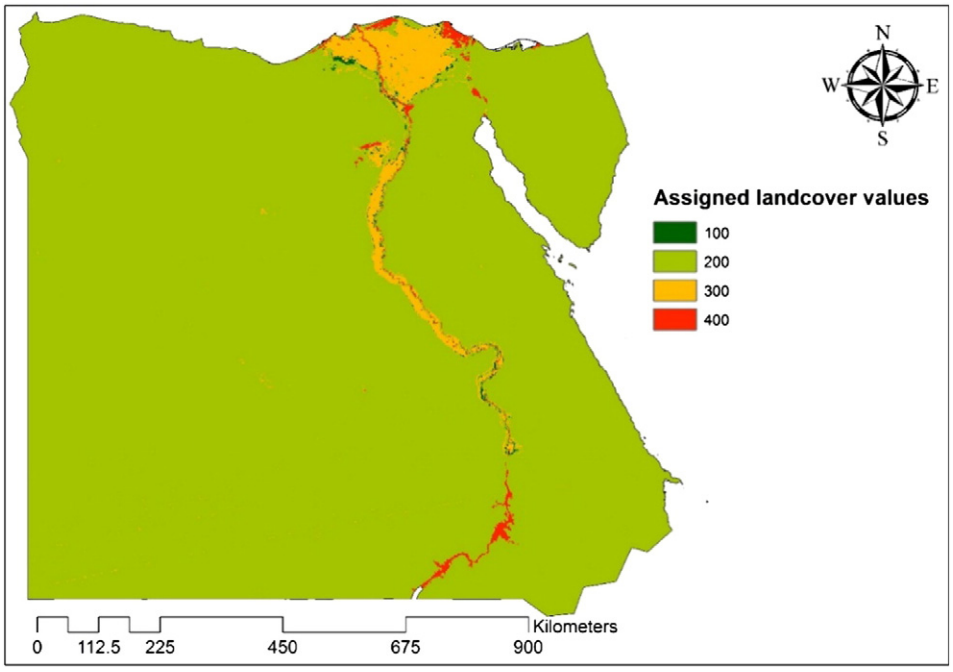


**Fig. 7.** Reclassified Landcover map.

total amount of rain does not exceed 1.8 billion $m^3$ per year. However, the average annual amount of rainfall water that is effectively utilized for agricultural purposes is estimated to be 1 billion $m^3$. Climatic data were obtained from the meteorological department, Ministry of Agriculture and interpolated by using the following sources:

1. Satellite images for monthly global precipitation from (1979 to 2009) obtained from the World Data Center for Meteorology.
2. NASA Tropical Rainfall Measuring Mission (TRMM) monthly global precipitation data from (1998–2010) obtained from NASA GES Distributed Active Archive Center.

The rainfall surplus (P-ET) map was calculated by subtracting long-term average monthly evapotranspiration values of the precipitation for all meteorological stations covering the period from 1950 to 2012. The annual rainfall surplus was calculated at each meteorological

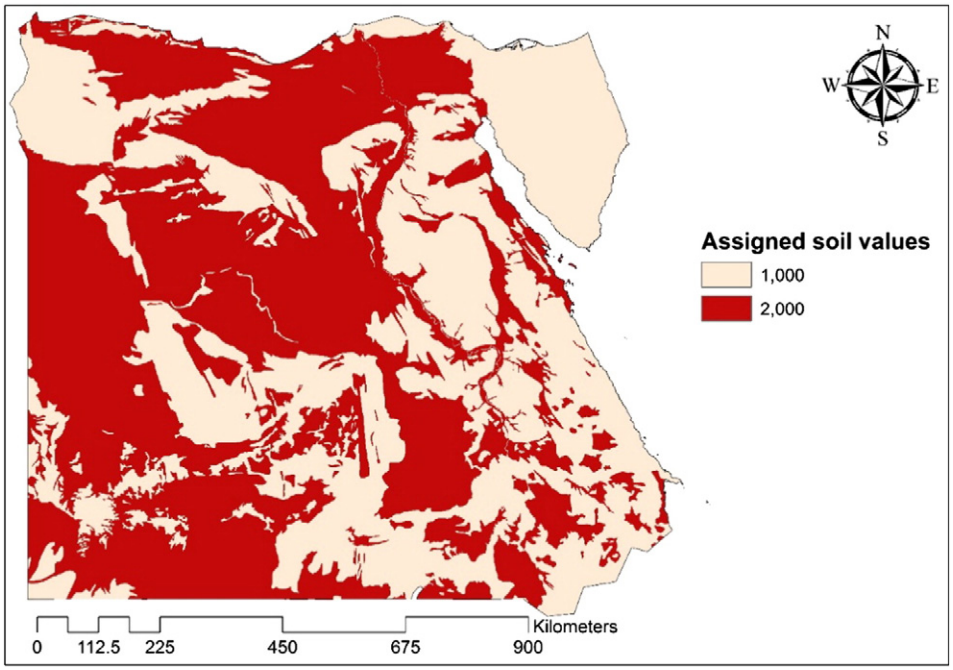


**Fig. 8.** Reclassified soil hydrological group map.

**Table 2**
Potential runoff coefficient for different land use, soil type and slope (Liu, 2004).

| Land use | Slope (%) | Sand | Loamy Sand | Sandy Loam | Loam | Silt Loam | Silt | Sandy clay Loam | Clay Loam | Silty clay Loam | Sandy Clay | Silty Clay | Clay |
|---|---|---|---|---|---|---|---|---|---|---|---|---|---|
| Forest | <0.5 | 0.03 | 0.07 | 0.10 | 0.13 | 0.17 | 0.20 | 0.23 | 0.27 | 0.30 | 0.33 | 0.37 | 0.40 |
| | 0.5–5 | 0.07 | 0.11 | 0.14 | 0.17 | 0.21 | 0.24 | 0.27 | 0.31 | 0.34 | 0.37 | 0.41 | 0.44 |
| | 5–10 | 0.13 | 0.17 | 0.20 | 0.23 | 0.27 | 0.30 | 0.33 | 0.37 | 0.40 | 0.43 | 0.47 | 0.50 |
| | >10 | 0.25 | 0.29 | 0.32 | 0.35 | 0.39 | 0.42 | 0.45 | 0.49 | 0.52 | 0.55 | 0.59 | 0.62 |
| Grass | <0.5 | 0.13 | 0.17 | 0.20 | 0.23 | 0.27 | 0.30 | 0.33 | 0.37 | 0.40 | 0.43 | 0.47 | 0.50 |
| | 0.5–5 | 0.17 | 0.21 | 0.24 | 0.27 | 0.31 | 0.34 | 0.37 | 0.41 | 0.44 | 0.47 | 0.51 | 0.54 |
| | 5–10 | 0.23 | 0.27 | 0.30 | 0.33 | 0.37 | 0.40 | 0.43 | 0.47 | 0.50 | 0.53 | 0.57 | 0.60 |
| | >10 | 0.35 | 0.39 | 0.42 | 0.45 | 0.49 | 0.52 | 0.55 | 0.59 | 0.62 | 0.65 | 0.69 | 0.72 |
| Crop | <0.5 | 0.23 | 0.27 | 0.30 | 0.33 | 0.37 | 0.40 | 0.43 | 0.47 | 0.50 | 0.53 | 0.57 | 0.60 |
| | 0.5–5 | 0.27 | 0.31 | 0.34 | 0.37 | 0.41 | 0.44 | 0.47 | 0.51 | 0.54 | 0.57 | 0.61 | 0.64 |
| | 5–10 | 0.33 | 0.37 | 0.40 | 0.43 | 0.47 | 0.50 | 0.53 | 0.57 | 0.60 | 0.63 | 0.67 | 0.70 |
| | >10 | 0.45 | 0.49 | 0.52 | 0.55 | 0.59 | 0.62 | 0.65 | 0.69 | 0.72 | 0.75 | 0.79 | 0.82 |
| Bare soil | <0.5 | 0.33 | 0.37 | 0.40 | 0.43 | 0.47 | 0.50 | 0.53 | 0.57 | 0.60 | 0.63 | 0.67 | 0.70 |
| | 0.5–5 | 0.37 | 0.41 | 0.44 | 0.47 | 0.51 | 0.54 | 0.57 | 0.61 | 0.64 | 0.67 | 0.71 | 0.74 |
| | 5–10 | 0.43 | 0.47 | 0.50 | 0.53 | 0.57 | 0.60 | 0.63 | 0.67 | 0.70 | 0.73 | 0.77 | 0.80 |
| | >10 | 0.55 | 0.59 | 0.62 | 0.65 | 0.69 | 0.72 | 0.75 | 0.79 | 0.82 | 0.85 | 0.89 | 0.92 |
| IMP | | 1.00 | 1.00 | 1.00 | 1.00 | 1.00 | 1.00 | 1.00 | 1.00 | 1.00 | 1.00 | 1.00 | 1.00 |

station by adding only the positive values of the difference (P-ET), spatial distribution of rainfall surplus map (Fig. 10) generated by interpolating previous data values using ArcGIS.

As noticed from Fig. 10, towards the South, rainfall tapers off very rapidly to less than 30 mm/year. It also fluctuates widely between years. One of the main issues is to increase the efficiency of runoff water use for human and animal consumption and cultivation, and to minimize soil erosion. This is possible because the area's geography and hydrology are ideal for effective use of water harvesting systems.

## 3. Rainfall–runoff modeling

Rainfall runoff relationships in the study area are considered using the SCS curve number method. In undertaking hydrological modeling using remote sensing data in GIS environment the SCS curve runoff model is largely suitable due to its reliance on land cover parameters, which can be extracted from RS (Senay and Verdin, 2004). This method has several advantages mostly based on its simplicity to apply and acceptability; however, the method is also associated with several disadvantages. This method nevertheless is found to be more appropriate in the absence of accurate hydrological and topographical data that is essential for runoff estimation (Senay and Verdin, 2004).

Runoff curve number estimates total storm runoff from total storm rainfall and this relationship excludes time as a variable and rainfall intensity. Its stability is ensured by the fact that runoff depth ($Q$) is bounded between 0 and the maximum rainfall depth ($P$). This implies that as rainfall amount increases the actual retention ($P - Q$) approaches a constant value, the maximum potential retention (USDA, 2004; Ponce and Hawkins, 1996). The runoff coefficient can be derived as either an event runoff coefficient or annual runoff coefficient. The event runoff coefficient is defined as the portion of rainfall that becomes direct runoff during an event. In hydrological modeling it represents the lumped effect of a number of processes in a catchment which may include: interception, evaporation, rainfall intensity, initial abstraction and hence runoff (Viglione et al., 2009).

## 4. Results and discussion

In this study, runoff curve number has been estimated based on the area's hydrologic soil group, land use, and slope. The soil map was classified into two classes; sandy and loamy soil. The loamy soil, which has a moderate infiltration rate when is thoroughly wetted, was classified as mainly or moderately deep infiltration, moderately to-well drained soils with moderately fine to moderately coarse textures. Sandy soil has the highest infiltration rate. These findings will lead to variations in runoff values since the soil texture is varied. From this result it can be depicted that loam soil is more suitable for runoff harvesting due to its lowest infiltration potential.

In Egypt, there is different land cover and land use classes where barren or sparsely vegetated land represents the largest ratio of the area 95.03% and 2.08% of the total area are irrigated cropland and pasture. Water bodies as shown in Table 1, represent 0.62% of the total area which are fixed sources. This percentage is not well distributed in the Egyptian territory.

The Egyptian territory comprises the following river basins:

- The Northern Interior Basin, covering 520,881 km$^2$ or 52% of the total area of the country in the east and southeast of the country. A subbasin of the Northern Interior Basin is the Qattara Depression.
- The Nile Basin, covering 326,751 km$^2$ (33%) in the central part of the country in the form of a broad north–south strip.
- The Mediterranean Coast Basin, covering 65,568 km$^2$ (6%).
- The Northeast Coast Basin, a narrow strip of 88,250 km$^2$ along the coast of the Red Sea (8%).

**Table 3**
Slope constant $S_0$ for determining potential runoff coefficient (Liu, 2004).

| Land use | Sand | Loamy Sand | Sandy Loam | Loam | Silt Loam | Silt | Sandy Clay Loam | Clay Loam | Silty Clay Loam | Sandy Clay | Silty Clay | Clay |
|---|---|---|---|---|---|---|---|---|---|---|---|---|
| Forest | 0.68 | 0.65 | 0.62 | 0.59 | 0.56 | 0.53 | 0.5 | 0.47 | 0.44 | 0.41 | 0.38 | 0.35 |
| Grass | 0.58 | 0.551 | 0.522 | 0.493 | 0.464 | 0.435 | 0.405 | 0.376 | 0.347 | 0.318 | 0.289 | 0.26 |
| Crop | 0.5 | 0.471 | 0.442 | 0.413 | 0.384 | 0.355 | 0.325 | 0.296 | 0.267 | 0.238 | 0.209 | 0.18 |
| Bare soil | 0.42 | 0.393 | 0.365 | 0.338 | 0.311 | 0.284 | 0.256 | 0.229 | 0.202 | 0.175 | 0.147 | 0.12 |

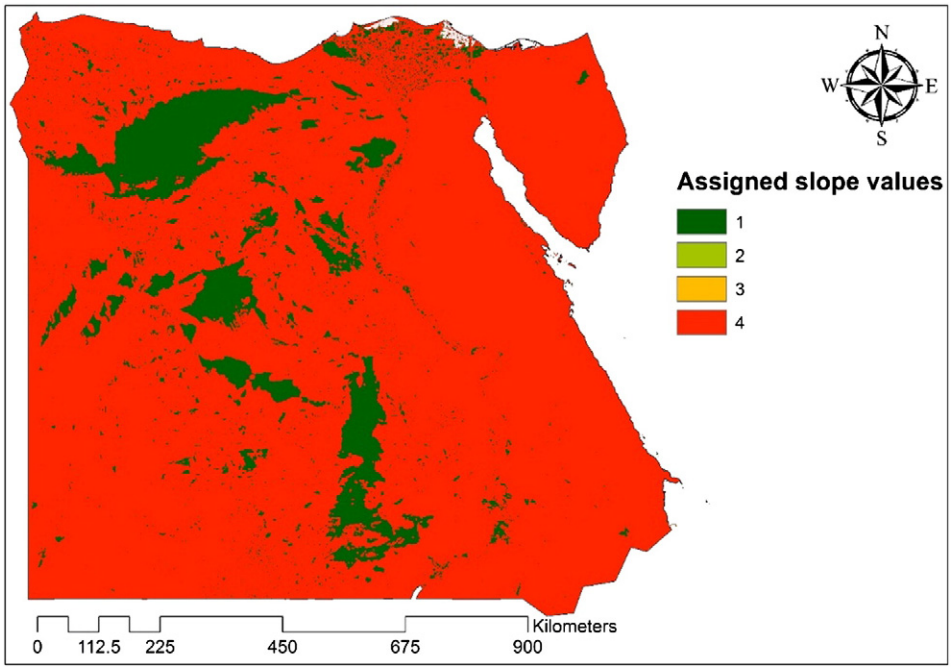


**Fig. 9.** Reclassified slope map.

As known, the River Nile is the main source of water in Egypt, with an annual allocated flow of 55.5 cubic kilometers per year ($km^3$/year) under the Nile Waters Agreement of 1959. In addition, the internal surface water resources are estimated as 0.5 $km^3$/year. Hence, this brings total actual surface water resources to 56 $km^3$/year. Moreover, the Nubian sandstone aquifer which is located under the Western Desert is considered an important groundwater source. Furthermore, the volume of groundwater entering the country from the Libyan Arab Jamahiriya is estimated at 1 $km^3$/year. Internal renewable groundwater resources are estimated at 1.3 $km^3$/year, bringing total renewable groundwater resources to 2.3 $km^3$/year. On the other hand, the main source of internal recharge is percolation from irrigation water in the valley and the delta. The modeled runoff coefficient developed by this study, which is presented in Fig. 11, shows a variation in the values of runoff from as low as 0.03 to a maximum of 1. These values indicate the potential amount of annual rainfall that can be harvested and used for agriculture, portable and groundwater recharge. Therefore, these harvested water can represent an additional water source in Egypt. Moreover areas with higher runoff potential are suitable locations to set up successful rainwater harvesting constructers to retain the water.

Many researchers in different parts of the world used runoff depth as an indication for mapping potential rainwater harvesting sites for

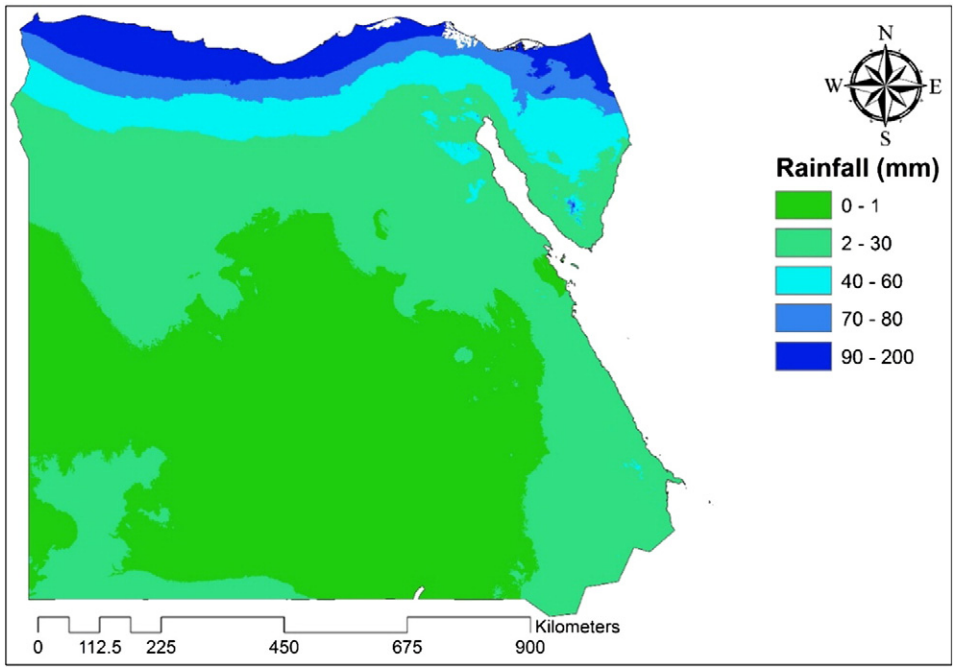


**Fig. 10.** Rainfall surplus map for the study area.

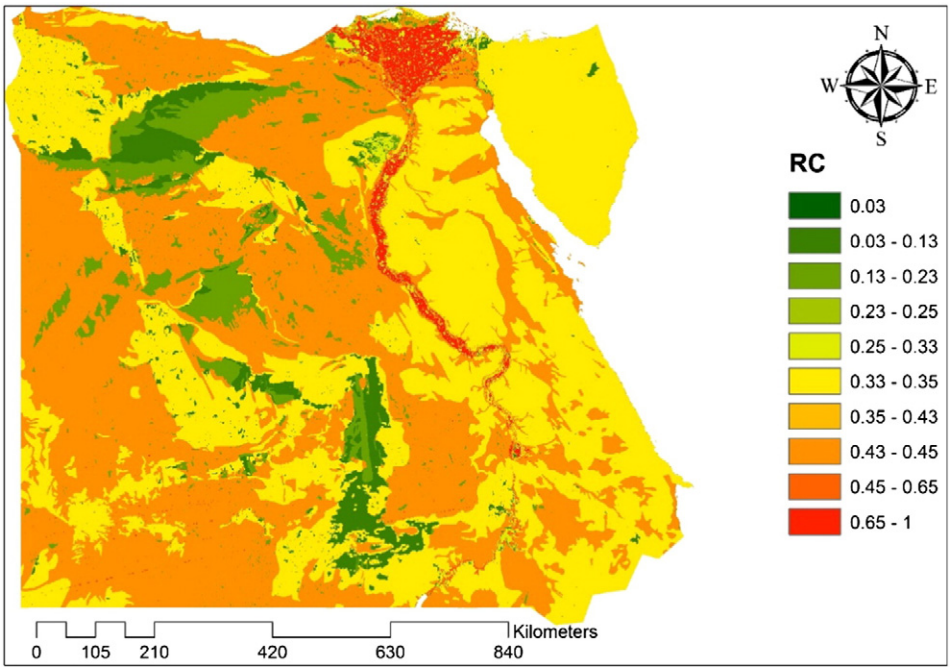


**Fig. 11.** Distribution of potential runoff coefficient.

different purposes. De Winnaar et al. (2007) used runoff depth for identifying the potential RWH potential sites for Thukela River Basin, South Africa. Ramakrishnan et al. (2008) used runoff potential as criteria to select suitable sites for various RWH/recharging structures in the Kali watershed, Dahod district of Gujarat of India, using remote sensing and GIS techniques. Durga Rao and Bhaumik (2003) identified runoff potential as criteria to identify suitable sites for RWH. While in Egypt there is a limited studied were done up to date in this area.

Annual runoff depth (Fig. 12) is derived for this study as opposed to event runoff coefficient for annual rainfall since establishing the runoff amount could be available for agricultural production. This method takes into account rainfall events that do not contribute significantly to any runoff. Annual runoff depth is derived using the annual rainfall surplus and runoff coefficient per pixel using the raster calculator tool in ArcGIS, which gives an indication of the rainfall percentage that, is transformed to runoff.

The results of spatial distributions of modeled annual runoff depth in mm are shown in Fig. 12. A variation from as low as 0 mm into a maximum of 180 mm was observed due to divergence in topography and climate in the study area, where the largest rainfall was observed in the

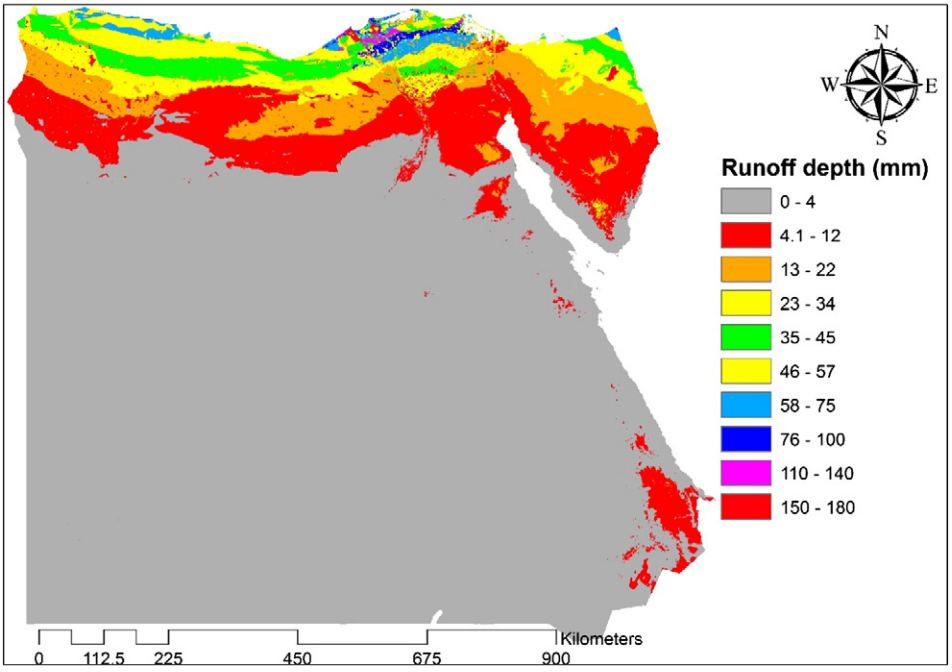


**Fig. 12.** Distributions of modeled annual runoff depth.

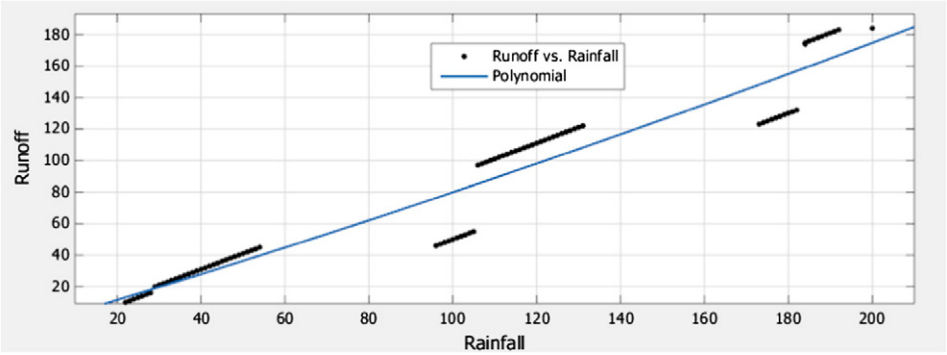


**Fig. 13.** Annual rainfall runoff relationship.

northern part. PRC, which is the ratio of modeled runoff depth to the annual rainfall, shows a wide variation over the study area.

The relationship shown in Fig. 13 gives an indication of how the satellite image derived rainfall amounts fit to the gauge measured rainfall. An indication that the absence of reliable ground measurements of rainfall product can satisfactorily be applied to estimate the spatial rainfall distribution based on the value of $R^2$ (0.9998) as obtained by linear modeling from Eq. (2). Despite the high correlations, one of the key problems may be the accuracy of the measured rainfall and its reliability. Annual runoff generation from the study area ranged from 3% to 100% of the total rainfall. This encourages the use of GIS and RS for environmental modeling in Egypt. Hence, rainfall data are not accurate, as it has to be due to the effect of dust-laden winds on the rain gauge.

Linear model Poly2:

$$F(x) = P_1 \times X^2 + P_2 \times X + P_3 \tag{2}$$

where $x$, is normalized by mean 85.34 and std 62.6Coefficients (with 95% confidence bounds):

$P_1 = 2.042(-1.371, 5.454)$
$P_2 = 55.18(52.21, 58.14)$
$P_3 = 66.85(62.49, 71.21)$

Goodness of fit:

SSE : 2.263e + 04
$R^2$ : 0.94.

Rainfall distribution in the study area shows the wise use of identifying suitable sites for rainwater harvesting where, most of the constructed dams are located in the higher rainfall areas. The same result was observed for runoff volume.

The effect of runoff–rainfall relationship with the environment, and the wise use of rainwater harvesting in any arid country such as Egypt, needs to be expanded to cover the entire country due its influence on understanding the water cycle and reduce flood risk as it always depends on runoff depth, especially in the very steep slope area.

## 5. Conclusion

It was shown clearly in this study that the remote sensing and GIS can provide the appropriate platform for convergent of large volume of multi-disciplinary data. Many regions of Egypt as well as of developing countries do not have sufficient historical records and detailed runoff information needed for physically based distributed models. In these cases, this study can provide a better solution for flood management programs. The used technique for determination of runoff coefficient is very useful in prediction/forecast of the temporal variation of the surface runoff at the outlet of the ungauged basin, which is useful in the hydrologic/environmental engineering applications. The described technique is economical and has high accuracy in determining the flood hydrograph for any area as it uses DEM of the area that can be freely accessed from SRTM or ASTER sources. Determination of runoff coefficient is important for flood control channel construction and for possible flood zone hazard delineation. A high runoff coefficient (C) value may indicate flash flooding areas during storms as water moves fast overland on its way to a river channel or a valley floor.

The large spatial variability in mean runoff coefficient, which ranges from 0.03 to 1, is relatively well explained by mean annual precipitation. Runoff coefficients tend to increase with mean annual precipitation. The significance of this relationship means that the mean annual precipitation influences the distribution of runoff coefficients not only through the characteristics of the flood-generating storm events, but also by controlling the variability of the initial conditions and, at longer time scales, likely by controlling the geomorphological structure of catchments, through soil formation and erosion processes.

Remote sensing data help tremendously in SCS-CN model as it serve as input for determination of drainage pattern, delineation of catchment, land use/land cover etc. which when integrated with GIS can be used in watershed management effectively. This work can be helpful for estimating runoff at places where observed runoff records are not available.

## 6. Recommendations

Since land use changes are so dynamic, images with better spatial and temporal resolution are recommended. Finer resolution data will significantly improve the classification accuracy. Satellite imagery should also be investigated as possible sources of all-weather land-cover data. The precipitation data which are obtained from the World Data Center for Meteorology, and NASA Tropical Rainfall Measuring Mission (TRMM), can be used in similar and further studies. In addition, this research could be taken a step farther by researcher in the future to determine the runoff curve number for other countries.

The high $R^2$ values obtained for the second degree polynomials fitted to annual rainfall–runoff indicate that the observed runoff and runoff estimated using the fitted equations are highly correlated. The fitted relationships will prove handy in estimation of annual/seasonal runoff for future annual/seasonal rainfall estimated using appropriate time series models, of course with a certain degree of reliability. This will help the water managers in charge of the operation of the lake to provide valuable information regarding water availability to farmers. Hence, the farmers can plan the schedule of the farming operations, the age and type of the crop to be grown and the extent of the cropping area in the particular crop season.

## References


American Society of Civil Engineers (ASCE), 1992. Design and Construction of Urban Stormwater Management Systems. American Society of Civil Engineers, New York, NY.

Browne, F.X., 1990. Stormwater management. Standard Handbook of Environmental Engineering RA Corbitt, 7 pp. 1–7 (135).

Cheng, Q., Ko, C., Yuan, Y., Ge, Y., Zhang, S., 2006. GIS modeling for predicting river runoff volume in ungauged drainages in the Greater Toronto Area, Canada. Comput. Geosci. 32 (8), 1108–1119.

Chow, V.T., Maidment, D.R., Larry, W. Mays, 1988. Applied Hydrology. McGrawHill International Editions.

De Winnaar, G., Jewitt, G.P.W., Horan, M., 2007. A GIS-based approach for identifying potential runoff harvesting sites in the Thukela River basin, South Africa. Phys. Chem. Earth A/B/C 32 (15), 1058–1067.

Durga Rao, K.H.V., Bhaumik, M.K., 2003. Spatial expert support system in selecting suitable sites for water harvesting structures — a case study of Song watershed, Uttaranchal, India. Geocarto Int. 18, 43–50.

FAO, 1974. FAO-UNESCO Soil Map of the World, 1:5.000.000. UNESCO, Paris.

FAO, 1978. Report on the agro-ecological zones project. World Soil Resources Report n. 48FAO, Rome.

Fetter Jr., C.W., 1980. Applied Hydrogeology. Charles E. Merrill and Co., Columbus, Ohio (484 pp).

Kirkby, M.J., Beven, K.J., 1979. A physically based, variable contributing area model of basin hydrology (Un modèle à base physique de zone d'appel variable de l'hydrologie du bassin versant). Hydrol. Sci. J. 24 (1), 43–69.

Liu, Y.B., 2004. Development and application of a GIS-based hydrological model for flood prediction and watershed management. VUB Hydrol. 46.

Liu, Y.B., De Smedt, F., 2004. WetSpa Extension, a GIS-based Hydrologic Model for Flood Prediction and Watershed Management. Vrije Universiteit Brussel, Belgium pp. 1–108.

Mallants, D., Feyen, J., 1990. Kwantitatieve en kwalitatieve aspecten van oppervlakte en grondwaterstroming (in Dutch). 2, 76 (KUL).

Ponce, V.M., Hawkins, R.H., 1996. Runoff curve number: has it reached maturity? J. Hydrol. Eng. 1 (1), 11–19.

Ramakrishnan, D., Bandyopadhyay, A., Kusuma, K.N., 2008. SCS-CN and GIS based approach for identifying potential water harvesting sites in the Kali Watershed, Mahi River Basin, India. J. Earth Syst. Sci. 118, 355–368 (No. 4, August 2009).

Senay, G.B., Verdin, J.P., 2004. Developing index maps of water-harvest potential in Africa. 20 (6), 789–799 (12).

Shereif, H., Mahmoud, F.S., Mohammad, Alazba, A.A., 2013. A GIS-based Approach for Determination of Potential Runoff Coefficient for Al-Baha Region, Saudi Arabia. IACSIT Press, Singapore pp. 97–102. http://dx.doi.org/10.7763/IPCBEE (V57 (19)).

Sherman, L., 1932. Stream flow from rainfall by unit hydrograph method. Eng. News Rec. 108, 501–505 (Chicago).

Sivapalan, M., Blo¨schl, G., Merz, R., Gutknecht, D., 2005. Linking flood frequency to long-term water balance: incorporating effects of seasonality. Water Resour. Res. 41 (6), W06012. http://dx.doi.org/10.1029/2004WR003439.

Texas Department of Transportation (TxDOT), 2002. Hydraulic Design Manual. TxDOT Hydraulics Branch of the Bridge Division, Austin, TX p. 78701.

USDA, 2004. Estimation of direct runoff from storm rainfall. National Engineering Handbook p. 79.

Viglione, A., Merz, R., Bloschl, G., 2009. On the role of the runoff coefficient in the mapping of rainfall to flood return periods. Hydrol. Earth Syst. Sci. 13.

Wanielista, M.P., Yousef, Y.A., 1993. Stormwater Management. John Wiley & Sons, Inc., New York.